Sodium-Ion Batteries: "Beyond Lithium-Ion"

M.Shirpour*, X. Zhan** and M. Doeff***

*University of Kentucky, Lexington, KY, USA, mona.shirpour@uky.edu
** University of Kentucky, Lexington, KY, USA, xiaowen.zhan@uky.edu
*** Lawrence Berkeley National Laboratory, Berkeley, CA, USA, mmdoeff@lbl.gov

ABSTRACT

Aqueous sodium-ion batteries may solve the cost and safety issues associated with the energy storage systems for the fluctuating supply of electricity based on solar and wind power. Aqueous, or water-based, sodium-ion batteries offer multiple cost savings using less expensive electrode materials and much cheaper electrolyte solutions compared to the lithium ion cells. In the present work, we for the first time report the electrochemical performance of $NaTi_2(PO_4)_3$ anode material paired with Na_2FePO_4F cathode material in an aqueous system. This aqueous sodium-ion battery exhibits a higher voltage and a greater specific energy (50 Wh/Kg) than its organic analog (45 Wh/Kg).

Keywords: sodium-ion battery, grid energy storage, abundant, low-cost, aqueous

1 INTRODUCTION

The drastic increase in demand for lithium-ion batteries in the electronics and automotive industries is currently putting enormous pressure on lithium supplies, and has resulted in a steep price rise for the lithium precursors used in the manufacture of electrode and electrolyte materials.[1] Sodium-ion batteries are an appealing lower cost alternative to lithium-ion batteries because of vast resources of sodium and much lower materials costs ($5000/ton for lithium in comparison with $160/ton for sodium).[2,3] Lithium is also a strategic element for energy because more than half of the world's lithium reserves are located in only three countries: Argentina, Bolivia, and Chile[4], while the United States has the world's largest deposits of sodium and is the lowest cost producer of sodium precursors. One-third of the world's sodium precursor comes from Wyoming's Green River Basin.[5]

Low cost energy storage systems are the key technologies for the fluctuating supply of electricity based on solar and wind power. Aqueous, or water-based, sodium-ion batteries are promising candidates for large-scale grid storage applications because they offer multiple cost savings using less expensive electrode materials, much cheaper electrolyte solutions compared to the lithium-ion cells, and less costly manufacturing conditions. They also have the extra advantage of being safer for grid applications,[6] and higher cycling efficiency due to the higher ionic conductivity of the aqueous electrolyte.

In the water-based cells, both the anode and cathode should undergo redox processes approximately within the voltage stability region of water (Figure 1a).

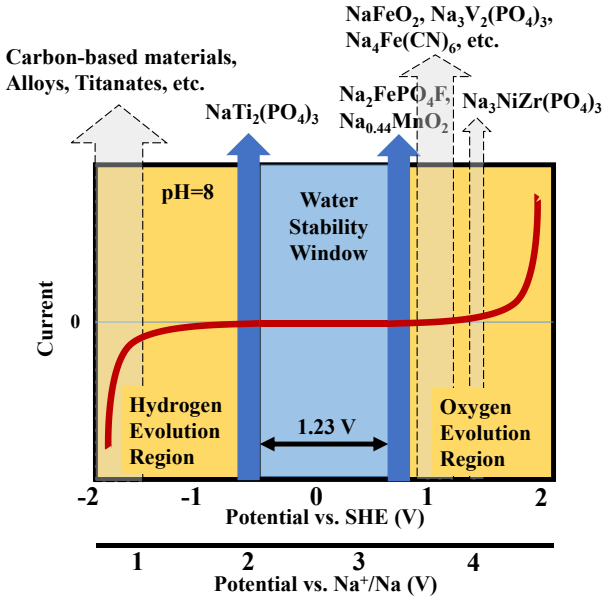

Figure 1: Voltage stability window of water; the highlighted regions show the operating voltage of most of the reported cathode and anode materials for sodium-ion cells.

Most of the anode materials [3,7,8] for sodium-ion batteries, including carbon-based compounds and titanates[9,10] have a very low operating voltage vs. sodium, and fall in the region of hydrogen evolution. NASICON ($NaTi_2(PO_3)_4$) as negative electrode and Na_2FePO_4F as positive electrode operate within the voltage stability region of water, 2.1 V and 3.0-3.2 V versus Na/Na^+, respectively. $NaTi_2(PO_3)_4$ accommodates 2 Na and exhibits a theoretical capacity of 133 mAh/g, and Na_2FePO_4F has a theoretical capacity of 124 mAh/g based on intercalation of one sodium.[3,6,8,11-13] These values correspond to a theoretical specific energy of 64 Wh/Kg based on the total weight of active electrode materials. In this work, we for the first time discuss aqueous sodium-ion batteries based on the combination of these two electrode materials. The

comparison between organic and aqueous electrolytes in this work highlights the potentials and limitations of water-based sodium-ion batteries.

2 EXPERIMENTAL

Synthesis and Electrode Fabrication: $NaTi_2(PO_4)_3$ and Na_2FePO_4F were prepared by solid state methods. For the $NaTi_2(PO_4)_3$ NASICON phase, a mixture of Na_2CO_3, TiO_2, and $6NH_4H_2PO_4$ was calcined at 800°C for 24 and at 1000°C for 12h, using intermediate milling and grinding (300rpm/2h). For the Na_2FePO_4F, a mixture of $Fe(C_2O_4).2H_2O$, $NaHCO_3$, NaF and $NH_4H_2PO_4$ was heated in an Alumina boat crucible at 350°C for 4h under Ar. Then dry milled for 4h at 100 rpm, and calcined at 600°C for 6h under Ar flow. Prior to electrode fabrication, the obtained active materials were milled with acetylene black (300rpm for 2h) in order to enhance the electronic conductivity of the electrodes. The electrodes were prepared by casting a mixture of the active materials, acetylene black and Polyvinylidene fluoride (PVDF) (in a weight ratio of 70:20:10 for positive electrode, and 70:25:5 for negative electrode) on aluminum foil for organic cells and on stainless steel foil for aqueous cells (Multipurpose 304 Stainless Steel Foil, Bright Finish, 0.001 inch thick).

Cells with Organic Electrolyte: Full sodium-ion cells with organic electrolyte were assembled using 2032-type coin cells inside in a helium-filled glovebox. Celgard 2400 was used as separators and 1M $NaPF_6$ (Sigma Aldrich) in EC:DMC (3:7 mol, from Novolyte Technologies) as the electrolytic solution.

Cells with Aqueous Electrolyte: Each electrode material was tested in a three electrode cell (Plate material evaluating cell from Bio-logic) with Pt foil counter electrode and Ag/AgCl (3 M NaCl) reference electrode. For full sodium-ion cells with aqueous electrolyte (1 M Na_2SO_4), the electrodes together with filter paper as separator were sealed in pouche cells. Electrochemical evaluation was carried out using a Bio-logic VMP3 potentiostat/galvanostat. Electrochemical impedance spectra were recorded from 100 kHz to 50 mHz.

3 RESULTS AND DISCUSSIONS

Our sodium-ion battery (full cell) consisting of $NaTi_2(PO_4)_3$ anode, Na_2FePO_4F cathode and organic electrolyte (1M $NaPF_6$ in EC/DMC) operates at about 0.9V with a reversible charge capacity of about 100 mAh/g cathode (Fig. 2), corresponding to a specific energy of about 45 Wh/Kg based on the total weight of active electrode materials. In the charge and discharge curves, there are two evident plateaus, indicating the redox reactions of Na_2FePO_4F.

When these two electrode materials (coated on stainless steel current collector instead of aluminum foil) are assembled in a pouch cell with aqueous electrolyte, similar features in the voltage profile are observed (Fig. 3a), which refer to similar intercalation mechanism of the sodium ions in both organic and aqueous systems. The specific capacity of the aqueous cell during the first and second cycles is about 90 mAh/g cathode, slightly lower than the reversible capacity of the organic cell (100 mAh/g). The voltage of the cell is slightly higher than the organic cell, most likely due to the smaller internal resistance in the aqueous system. The cell capacity of 90 mAh/g and potential of 1.1 V correspond to a specific energy of about 50 Wh/Kg based on the total weight of active materials.

Despite these similarities for the first few cycles, the capacity of the aqueous cell drops significantly, and goes down to 50% of the initial capacity on the 15th cycle (Fig. 3b). The fast capacity fade in aqueous lithium- and sodium-ion batteries has often been reported.[7,14-17] The mechanism responsible for this severe capacity fading upon cycling has not been clarified.

In order to learn about the mechanism of capacity loss, we studied the positive and negative electrode materials separately, using a three electrode cell with Ag/AgCl reference electrode.

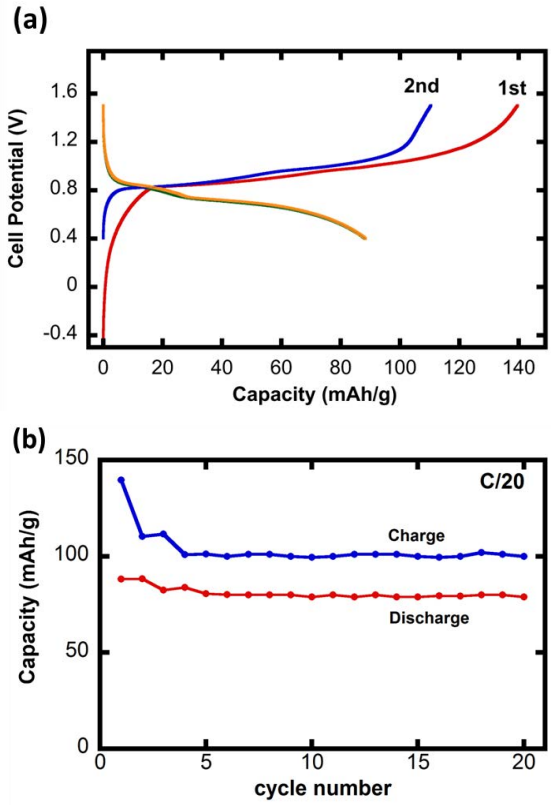

Figure 2: Electrochemical performance of a sodium-ion battery with $NaTi_2(PO_4)_3$ anode, Na_2FePO_4F cathode, and organic electrolyte cycled between 0.4 V and 1.5 V at 0.027 mA/cm^2.

Electrochemical performance of $NaTi_2(PO_4)_3$ at different C-rates in aqueous three-electrode cells is shown

in Fig. 4a. At 5C, the plateau at -0.5V vs. Ag/AgCl suggests that electrochemical side reactions happen during the cell discharge. At higher C-rates i.e. 20C and 50C, the extra voltage plateau does not exist. Therefore, at slower charge/discharge rates the side reactions are eliminated or happen more slowly. The electrochemical impedance spectra of the assembled cells before cycling is shown in Fig. 4b. We did not observe any high frequency semicircle in the initial spectra of the as-made cells, but the impedance spectra of the cycled cells consist of one semicircle at high frequency range (Fig. 4c).

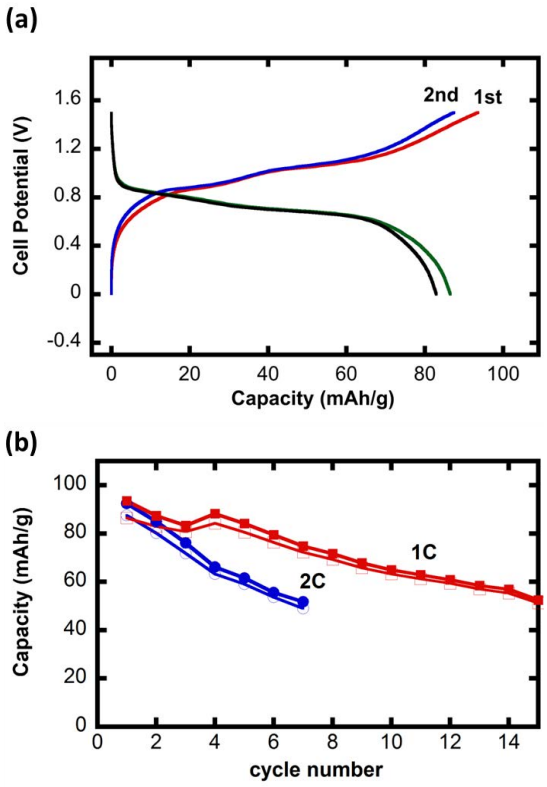

Figure 3: Electrochemical performance of sodium-ion batteries with $NaTi_2(PO_4)_3$ anode, Na_2FePO_4F cathode, and aqueous electrolyte (a) Voltage profile for the cell cycled between 0 V and 1.5 V at 0.21 mA/cm^2, (b) Capacity vs. cycle number for cells cycled at 1C (0.21 mA/cm^2) and 2C (0.42 mA/cm^2).

Formation of surface electrolyte interface (SEI) layer in non-aqueous lithium-ion batteries is a common observation and the high frequency semicircle is usually assigned to the diffusion of lithium ions through this SEI layer. In aqueous electrolytes, the formation of SEI is not extensively proved. It is reported that SEI layer is not formed in the presence of aqueous electrolytes, or even if it is formed the resistance of such an ultra-thin layer is negligible. Our results show that the size of the high frequency semicircle decreases at higher charge/discharge rates, and according to our electrochemical measurements side reactions are less pronounced at higher charge/discharge rates. Therefore, the high frequency semicircle originates from the products of the side reaction, and its size changes with the thickness of the surface layer. We see a better capacity retention for the 1C compared to the 2C (Fig. 3b), therefore the surface layer, similar to the SEI layer, could act as a protective barrier between the anode and the electrolyte.

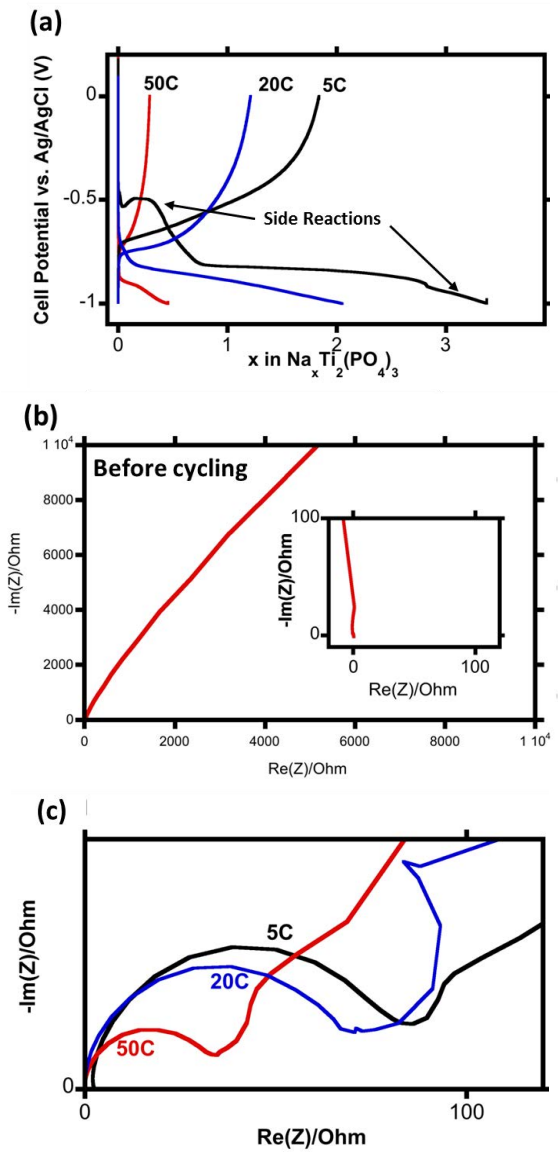

Figure 4: (a) Voltage profile of the $NaTi_2(PO_4)_3$ cycled in aqueous electrolyte between -1V and 0 V vs. Ag/AgCl at different C-rates. (b) Nyquist plots of the cells before cycling. (c) Nyquist plots of the cells after 20 cycles.

Similar measurements on Na_2FePO_4F positive electrodes in aqueous three-electrode cells were performed (Fig. 5a). At C/20 there was an additional, relatively large, plateau at around 0V vs. Ag/AgCl. This plateau became smaller at slower rates. Our conclusion is that side reactions

are eliminated or postponed in faster charge/discharge rates. Similarly, a high frequency semicircle formed after the cycling, and the size of this semicircle chnages with the charge/discharge rate and side reactions.

Based on our high resolution synchrotron XRD measurements (not shown here) the electrode compounds do not decompose during the cycling, and remain crystalline. We are currently studying the composition of the electrode surface using XPS which is a highly surface sensitive technique.

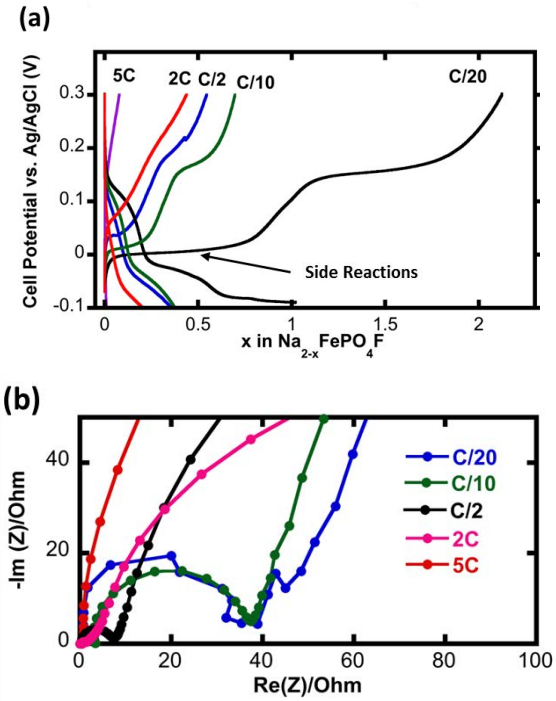

Figure 5: (a) Voltage profile of the Na_2FePO_4F cycled in aqueous electrolyte between -0.1V and 0.3 V vs. Ag/AgCl at diffrenet C-rates. (b) Nyquist plots of the cells after 20 cycles.

Strategies for improvement of cyclability in aqueous sodium-ion batteries are essential for implementation of these batteries in grid-scale storage. Our most recent experiments show enhancement of cycling behavior in $Na_{0.44}MnO_2$ cathode material by partial substitution of Mn with Ti.

4 CONCLUSIONS

We have developed an aqueous sodium-ion battery based on a NASICON-type anode material, and a fluorophosphate cathode material. The specific energy of the cell is 50Wh/Kg, which is larger than the specific energy of similar cell with organic electrolyte. The higher specific energy is mainly due to the lower electrolyte resistance, and therefore higher cell voltage. The similarities between the organic and aqueous systems suggest that the electrochemical reactions of electrodes in organic cells are valid in the aqueous systems. The electrochemical impedance data show that irreversible side reactions in slow cycling rates result in formation of a protective layer on both negative and positive electrodes.

5 ACKNOWLEDGMENTS

This work was supported by the Laboratory Directed Research and Development Program of Lawrence Berkeley National Laboratory under U.S. Department of Energy Contract DE-AC02- 05CH11231, and Department of Chemical and Materials Engineering at the University of Kentucky.

REFERENCES

[1] Wu, C. MRS Bulletin 2010, 35, 650.
[2] Ellis, B. L.; Nazar, L. F. Current Opinion in Solid State and Materials Science 2012, 16, 168.
[3] Palomares, V.; Serras, P.; Villaluenga, I.; Hueso, K. B.; Carretero-Gonzalez, J.; Rojo, T. Energy & Environmental Science 2012, 5, 5884.
[4] USGS (United States Geological Survey), http://minerals.usgs.gov/minerals/pubs/commodity.
[5] WSGS (Wyoming State Geological Survey), http://www.wsgs.uwyo.edu.
[6] Li, Z.; Young, D.; Xiang, K.; Carter, W. C.; Chiang, Y.-M. Advanced Energy Materials 2013, 3, 290.
[7] Kim, H.; Hong, J.; Park, K. Y.; Kim, H.; Kim, S. W.; Kang, K. Chemical Reviews 2014, 114, 11788.
[8] Slater, M. D.; Kim, D.; Lee, E.; Johnson, C. S. Advanced Functional Materials 2013, 23, 947.
[9] Shirpour, M.; Cabana, J.; Doeff, M. Energy & Environmental Science 2013, 6, 2538.
[10] Shirpour, M.; Cabana, J.; Doeff, M. Chemistry of Materials 2014, 26, 2502.
[11] Park, S. I.; Gocheva, I.; Okada, S.; Yamaki, J.-i. Journal of The Electrochemical Society 2011, 158, A1067.
[12] Kawabe, Y.; Yabuuchi, N.; Kajiyama, M.; Fukuhara, N.; Inamasu, T.; Okuyama, R.; Nakai, I.; Komaba, S. Electrochemistry Communications 2011, 13, 1225.
[13] Il Park, S.; Gocheva, I.; Okada, S.; Yamaki, J. Journal of the Electrochemical Society 2011, 158, A1067.
[14] Wu, W.; Mohamed, A.; Whitacre, J. F. Journal of the Electrochemical Society 2013, 160, A497.
[15] Wang, G. J.; Fu, L. J.; Zhao, N. H.; Yang, L. C.; Wu, Y. P.; Wu, H. Q. Angewandte Chemie-International Edition 2007, 46, 295.
[16] Li, Z.; Young, D.; Xiang, K.; Carter, W. C.; Chiang, Y. M. Advanced Energy Materials 2013, 3, 290.
[17] Luo, J. Y.; Cui, W. J.; He, P.; Xia, Y. Y. Nature Chemistry 2010, 2, 760.